A Computational Modeling Study on Nanorefrigerants: Definition of Miscellaneous Multiplier M

MeldaOzdincCarpinlioglu[1*]Mahmut Kaplan[2]

1_Department of Mechanical Engineering, Gaziantep University, Gaziantep, Türkiye_
2Department of Machine and Metal Technology, Gaziantep University, Gaziantep, Türkiye
Corresponding Author:MeldaOzdincCarpinlioglu

---ABSTRACT---
The selected experimental data from researches on performance of refrigeration systems handling NRF (Al$_2$O$_3$-R134a) with the ranges of d$_p$= 20-70 nm, φ = 0.075-0.303%, V = 6.5-11 liter/hour, T$_e$= 288-309 K and T$_o$ = 294-306 K are used. The data are expressed through functional relationships of relative unitless parameters of COP$_r$, k$_r$, μ$_r$, ρ$_r$, c$_{p_r}$, h/d$_p$, T$_o$/T$_e$, φ, k$_p$/k$_R$.As a result of correlation trials Miscellaneous Multiplier is defined as M = [h/d$_p$]$^{1.95}$[T$_o$/T$_e$]$^{5.5}$[ln(k$_p$)/k$_R$]$^{1.45}$[k$_r$] [ρ$_r$]$^{0.5}$[c$_{p_r}$][-4.967(φ)^2 + 1.408 (φ)] independent of V. The validity of proposed equation of COP$_r$(M) is in the order of ±5%. The applicability of COP$_r$(M) is verified under the influence of nanoparticle, R type and varying T$_e$. It seems that type of nanoparticle and φ are the governing parameters for the magnitude of M. The critical range of φ seems to be 0.025-0.26% providing the optimum situation in a refrigeration system with a maximum COP$_r$. Definition of Miscellaneous Multiplier, proposed COP$_r$(M), COP$_r$(φ) are the primary contributions.
KEYWORDS;_Nanorefrigerant, computational modelling, relative coefficient of performance, model, miscellaneous multiplier_

Date of Submission: 30-07-2022   Date of Acceptance: 28-08-2022

I. INTRODUCTION

A computational modeling study is conducted as a contribution to the state of art on nanorefrigerants, NRF.The study is founded on a description of a parameter set of nanoparticle, refrigerant, R and NRF. Thermophysical characteristics; thermal conductivity, k, dynamic viscosity, $μ$, material density, $ρ$, specific heat, $c_p$and the size of nanoparticles, d_p, capping layer thickness, h, nanoparticle volume fraction,$φ$, and reference - ambient temperature, T_o are considered. The provided enhancement on cooling capacity of a refrigeration system is described by the major system operational parameters of coefficient of performance, COP, volumetric flow rate of NRF, V and evaporator temperature, T_e.

Nanorefrigerants, NRF are the colloidal suspension of nano-sized (1-100 nm) metals, metal oxides, metal carbides, carbon, grapheme, and hybrid materials [1] utilized in the form of particles, tubes, sheets in a variety of refrigerants, R used as the heat absorber or cooling agents [2, 3]. NRF can be classified as conventional chlorofluorocarbons (CFC) based (R11, R12 and R13)ones and alternative; hydrochlorofluorocarbon (HCFC) based (R123, R122) and HFC based (R134a) halogen free based (R600a, ammonia) ones [4, 5].The primary advantage of NRF is on the increased lifetime of handling systems particularly due to their improved solubility with lubricants [6].

NRF are also preferred for their superior friction coefficient and wear rate characteristics over those of pure R. NRF have a great potential to improve heat transfer mechanisms in vapor compression systems (VCS) due to the enhancement ofthermophysical characteristics of pure R [7].The material type, shape, and particularly size which is sensed by diameter $d_p$besides thermal conductivity, k, density, $ρ$ and specific heat, $c_p$are the major nanoparticle material parameters. The parameters belonging to the preparation methodology are nanoparticle volume fraction, $φ$, temperature, $T$and presence, type and amount of additives besides extraordinary technological constraints.

Thermophysical characteristics of R and NRF are thermal conductivity, k, dynamic viscosity, $μ$, density,$ρ$and specific heat, c_p. Operational parameters are T_e, T_o,amount of R – NRF circulating V independent of system and equipment design characteristics. Coefficient of performance, COP is obviously the preferred operational system parameter defined as follows:

$$COP = \frac{\text{Refrigeration effect } (Q_{evap})}{\text{Power input to compressor} (W_{comp})} \quad (1)$$

The presence of nanoparticles causes a significant change in thermophysical characteristics of R which is associated with a corresponding influence on system COP.Therefore a relative COP term can be defined for comparison purpose as follows:

$$COP_r = COP_{NRF}/COP_R \quad (1a)$$

$$r = NRF/R \quad (1b)$$

Thermophysical characteristics of NRF are the topic of experimental studies between 2009 and 2020 [8-16]and of theoretical studies providing estimations between 2009 and 2020 [8, 13-20]. The available experimental research focusing on the operational performance of refrigeration systems using NRF is between 2015 and 2020 [21-23].There are only a few numerical studies published between 2015 and 2019 on predicting COP of systems using NRF [17-18, 24]. In these studies, COP of the refrigeration systems is determined using existing correlations related to thermophysical characteristics of NRF [17, 18] and calculation of NRF enthalpies at various evaporation and condensation T [24]. However these models are not validated by experimental data.

II. STATE OF ART

The literature review is given in terms of experimental and theoretical approaches on thermophysical characteristics and on the cooling system performance to determine the perspectives given in session 3 which form the basis of the computational modeling study.

2.1 Experimental studies on thermal conductivity, viscosity, density and specific heat of NRF

The thermophysical characteristics of the nanoparticles and R referred from summarized literature are presented in Table 1 and 2, respectively.Experimental studies show that k NRF is higher than k_R[8-16]. This is due to the remarkably higher magnitudes of particle thermal conductivity, k_p(Table 1 and Table 2). Therefore, suspending nanoparticles in R enhances the heat transfer performance and reduces the energy consumption in comparison to that of R.The available experimental studies conducted on the enhancement of k, μ, and ρ of NRF by considering the influence of d_p, φ and T are given in Table 3.

Nanoparticles	k (W/mK)	ρ (kg/m^3)	c_p(J/kgK)	References
Al$_2$O$_3$	40	3880	729	Alawi et al. [18]
CuO	20	6500	535.6	Alawi and Sidik [15]
SiO$_2$	1.2	2200	703	Zarma et al. [25]
TiO$_2$	11.7	4260	689	Reddy and Rao [26]
Al	237	2700	877	Murshed [27]
Cu	383	8954	386	Lahari et al. [28]
Ni	90.7	8900	444	Salehi et al. [29]
SWCNT	2000	2200	709	Alawi and Sidik [19]

Table 1: The cited thermophysical characteristics of nanoparticles

Refrigerants	k (W/mK)	μ (mPas)	ρ (kg/m^3)	c_p(J/kgK)	References
R11	0.08740	0,47055	1479.05	884.6	Diao et al. [30]
R113	0.06517	0.5375	1527	932.5	Alawi et al. [3]
R123	0.07586	0.40805	1458.8	1022	Alawi et al. [31]
R134a	0.08030	0.1905	1199.7	1432	Mahbubul [32]
R141b	0.09205	0.4327	1243.4	1147	Alawi et al. [18]

Table 2:The cited thermophysical characteristics of base refrigerants

Refrigerants	Nanoparticle	d_p(nm)	φ(%)	T (K)	Max k(%)	Max μ(%)	Max ρ(%)	References
R11	Al$_2$O$_3$	20	0.01-0.05	289	-	19	-	[14]
	Al$_2$O$_3$	20	0.23-1.08		20	-	-	
	CuO	40	0.23-1.08		22	-	-	
R113	Al	18	0.20-1.00	303	22	-	-	[8]
	Cu	25	0.20-0.91		25	-	-	
	Ni	20	0.18-0.96		18	-	-	
R113	CNT	15	0.2-1.0	303	104	-	-	[9]
R123	TiO$_2$	21	0.5-2	298	-	5	-	[13]
R141b	Al$_2$O$_3$	13	0.1-0.4	293	2	1	1	[10]
	Al$_2$O$_3$	20-30			11	-	-	
R141b	SiO$_2$	30-50	0.02-0.1	298	13	-	-	[12]
	TiO$_2$	25-40			12	-	-	
	Al$_2$O$_3$	10-15			33	-	-	
R141b	SiO$_2$	20	0.0-0.6	298	30	-	-	[16]
	TiO$_2$	15-25			32	-	-	

Table 3:Summary of experimental studies conducted on thermophysical characteristics of NRF

Jiang et al. [8] examined k (NRF: Cu, Al, Ni, CuO and Al2O3-R113). Their experimental results revealed that k NRF with various nanoparticles improved with an increase in φ. There are various factors affecting k such as Brownian motion, T, nanoparticle material, size and shape [33, 34]. Jiang et al. [9] examined k (NRF: CNT –R113) having dp range (15-80 nm) and an aspect ratio range (18.8-666.7). They concluded that CNT with smaller dp (15 nm) and higher aspect ratio (666.7) intensified k (NRF: CNT-R113).

Mahbubul et al. [10] found that k (*NRF*: Al$_2$O$_3$ (13 nm)-R-141b) increased with an increase of φ (0.1-0.4%) and increase in T (278-293 K). Zhang et al. [12] studied k (NRF: Al$_2$O$_3$(20-30 nm), SiO$_2$(30-50 nm) and TiO$_2$(25-40 nm)-R141b) containing nanoparticles with low φ (0.02-0.10%). They reported that the increase in φ and T augmented k NRF.It is known that μ indicates not only the resistance of a fluid to flow in link with pressure drop and pumping power in the refrigeration system but also has a significant impact on heat transfer mechanism. Therefore μ NRF has an apparent effect on COP. Mahbubul et al. [13] investigated the influence φ and T on μ(NRF: TiO$_2$-R123) considering the ranges T (278-293 K) and φ (0.5-2%). It was found that μ NRF increased with an increase of φ and decreased with an increase in T.

Moreover, the augmentation in μ with increasing nanoparticle concentration augmented pressure drop with NRF. Therefore, low φ is recommended for a better refrigeration system performance. Dhindsa and Kundan[14] observed μ (NRF: Al$_2$O$_3$ (20 nm)-R11) with varying φ (0.01-0.05%) for a T range (277-289 K). They found that μ augmented significantly with an increase in φ. Mahbubul et al. [10] investigated the influence φ and T on μ (NRF: Al$_2$O$_3$ (13 nm)-R141b) considering the ranges of T (278 to 293 K) and φ (0.1-0.4 %). They reported that μ increased with an increase in φ and decreased with an increase in T. Since the increase of μ NRF generally resulted in a higher pressure drop, an optimum φ is required to augment the performance of the refrigeration systems[35, 36].It can be estimated that ρ and $c_p$of NRF also influence heat transfer performance of the refrigeration system. ρNRF is greater than ρ R as a function of φ. As is given in [10],ρ (NRF: Al$_2$O$_3$ (13 nm)-R141b) is increased by increasing φ from 0.1 to 0.4% at T= 293 K. Although there is almost no experimental study concerning c_pNRF, it is said that adding nanoparticles into a base fluid such as water and ethylene glycol causing a reduction in c_p of base fluid if $c_p$of the nanoparticles is lesser than $c_p$of base fluid [26].

Alawi and Sidik[15]investigated $c_p$behaviour of CuO-R134a NRF when φ ranges from 1 to 5% at 300-325 K T by calculating c_p NRF using the model proposed by Pak and Cho [37]. Similarly, Alawi and Sidik[19] examined the influence of φ onc_p of SWCNT-R134a NRF for the φ of (1 to 5%) at T of (300 to 320 K) by using the Pak and Cho model. It was concluded that c_p increased by increasing nanorefrigerant$T$ and decreased by increasing φ of CuO and SWCNT. Therefore a decrease of c_p NRF is a fact.

The available experimental studies conducted on the enhancement of k, μ, and ρ of NRF by considering the influence of d_p, φ and T are given in Table 3. The covered ranges for φ, T and$d_p$are (0.01-2 %), (289-303 K) and (13-50 nm) respectively. The given enhancement in$k$, μ, and ρ are (2-104%), (1-19%) and 1% [10]respectively. The highest k enhancement is obtained with CNT-R113. Similarly, Cu-R113 exhibits higher k enhancement compared to other sphere shaped nano particles (Al$_2$O$_3$, CuO, Al, and Ni) in R113 at approximatelythe same φ and T. This is possibly due to the high magnitudes of k CNT and k Cu among the others (Table 1).

2.2 Available theoretical models for thermal conductivity and viscosity of NRF
As a review dating back to 1881's Table 4 and Table 5 are installed to show a summary of available models for estimating k and μ of NRF respectively in terms of relative unitless parameters of k_r and μ_r defined as follows:

$$k_r = \frac{k_{NRF}}{k_R}, \quad \mu_r = \frac{\mu_{NRF}}{\mu_R} \quad (2)$$

Jiang et al. [8] developed a new model based on particle aggregation theory. It was concluded that their model had a good generalization capability for predicting k NRF: (Al (18 nm), Cu (25 nm), Ni (20 nm), Al$_2$O$_3$ (20 nm), and CuO (40 nm)-R113) for φ (0.18-1.08%) at T = 303 K. Besides, Mahbubul et al. [10] used the models proposed by Maxwell [38] and Sitprasert et al. [40] to estimate k NRF (Al$_2$O$_3$ (13 nm)-R141b) for φ (0.1-0.4%) at T = 293 K. The mean deviation was 0.1% and 1.38% with Maxwell and Sitprasert et al. models, respectively. Molana and Wang [20]proposed a new model to predict k NRF as a function of k_p, φ, $d_p$and T using the Gauss-Newton multiple regression scheme. They compared their numerical result with the experimental study conducted by Mahbubul et al. [11] for NRF: Al$_2$O$_3$-R141b with φ = 0.5-2% and T = 278-298 K. They concluded that k NRF increased with T for experimental and predicted data. Zhang et al. [12]suggested a model considering the mechanisms of interfacial layer, aggregation and Brownian motion to predict k NRF: (Al$_2$O$_3$ (20-30nm), SiO$_2$ (30-50 nm), TiO$_2$ (25-40 nm)-R141b) for φ = 0.02−0.1% and T = 278−298 K. They concluded that the calculated values of k NRF are in good agreement with the experimental ones, with a deviation less than 3%.

Alawi and Sidik[15]estimated k and μ (NRF: CuO (20 nm)-R134a) for φ (1-5%) at T = 300-325 K by using the models suggested by Ko and Kleinstreuer[39]and Tiwari and Das [45], respectively. They stated that k NRF increased by an increase of T and φ. They found that μ NRF decreased with an increase of T and a decrease of φ. Alawi and Sidik[19]used Ko and Kleinstreuer model and Tiwari and Das model to determine k and μ NRF: (SWCNT-R-134a) for φ (1-5%) at T = 300-320 K. Their results indicated that k and μ of *NRF* increased with the increase of φ. k NRF increased and μ NRF decreased by increasing T.Mahbubul et al. [11]investigated μ NRF: (Al$_2$O$_3$-R141b) for φ (0.5-2.0%) at T = 273 K. Their measured μ was found to be significantly higher compared to μ gained using the model proposed by Brinkman [42].Mahbubul et al. [13] compared their experimental results including μ NRF: (TiO$_2$-R123) upto a maximum φ = 2% at T = 298-300 K with the models proposed by Einstein [41], Batchelor[43] and Chen et al. [44]. They concluded that their experimental results were nearly same with the results obtained by Batchelor and Chen et al. models while μ obtained using Einstein model was lowfor the volume fraction bigger than 1 %.

Researchers	Models
Maxwell [38]	$k_r = \dfrac{2k_R + 2(k_p - k_R)\varphi + k_p}{2k_R - (k_p - k_R)\varphi + k_p}$
Ko and Kleinstreuer[39]	$k_r = \dfrac{2k_R + 2(k_p - k_R)\varphi + k_p}{2k_R - (k_p - k_R)\varphi + k_p} + \dfrac{5 \times 10^4 \beta \rho_R c_{p_R} \varphi}{k_R} \sqrt{\dfrac{k_b T}{\rho_p d_p}} f(T, \varphi)$
Jiang et al. [8]	$k_r = \dfrac{2L_x L_{layer} \sum\limits_{j=1}^{n_{ny}} \sum\limits_{k=1}^{n_{nz}} \left(k_{1,j,k} \left(T_{high} - T_{1,j,k} \right) \right)}{k_R L_y L_z \left(T_{high} - T_{low} \right)}$ L = side length of unit cube cell, L_{layer} = thickness of adsorbtion layer of particle
Sitprasert et al. [40]	$k_r = \dfrac{(k_p - k_l)\varphi k_l \left[2\beta_1^3 - \beta^3 + 1 \right] + (k_p + 2k_l)\beta_1^3 \left[\varphi \beta^3 (k_l - k_R) + k_R \right]}{\beta_1^3 (k_p + 2k_l) - (k_p - k_l)\varphi k \left[\beta_1^3 + \beta^3 - 1 \right]}$ $\beta = 1 + \dfrac{2t}{d_p}, \ \beta_1 = 1 + \dfrac{t}{d_p}, \ t = 0.01(T - 273)\left(\dfrac{d_p}{2}\right)^{0.35}$
Molana and Wang [20]	$k_r = \left(1 + 0.00033 k_p^{0.06} \varphi^{0.14} T^{1.5} \dfrac{1}{d_p^{0.11}} \right)$
Zhang et al. [12]	$k_r = \left(1 + A \operatorname{Re}_a^m \operatorname{Pr}^{0.333} \varphi_a \right) \left[\dfrac{k_a + 2k_R + 2\varphi_a (k_a - k_R)}{k_a + 2k_R - \varphi_a (k_a - k_R)} \right]$ A = emprical constant, m = emprical constant, a = aggregate

Table 4: Available models for k_r

Researchers	Models
Einstein[41]	$\mu_r = 1 + 2.5\varphi$
Brinkman [42]	$\mu_r = \dfrac{1}{(\varphi - 1)^{2.5}}$
Batchelor[43]	$\mu_r = 1 + 2.5\varphi + 6.5\varphi^2$
Chen et al. [44]	$\mu_r = \left[1 - (\varphi_a - \varphi_m) \right]^{-2.5\varphi_m}, \ \varphi_a = \varphi(a_a/a)^{3-D}, \ a_a$ = radius of aggregate, a = radius of primary particles, D = fractal index
Tiwari and Das [45]	$\mu_r = \dfrac{1}{1 - 34.87 \left(\dfrac{d_p}{d_R}\right)^{-0.3} \varphi^{1.03}}$

Table 5: Available models for μ_r

As an alternative approach for the determination of k_r and μ_r a recent study [46] of the authors published in 2021 should be outlined here. Available experimental data of relevant literature were evaluated in terms of second order polynomial regression analysis of the commercial software MATLAB. The selected data of

EG/EG-W based nanofluids for φ ≤ 10% with d_p= 10-100 nmat a *T* range of 293.15-323.15 K were fitted to an equation for calculating $k_r$as follows:

$$k_r = \mathrm{B}\left(-0.0005877\varphi^2 + 0.04623\varphi\right) + 1.008 \quad (3a)$$

The selected data of EG/EG-W based nanofluids for φ ≤ 9% with d_p= 7-100 nm and a *T* range of 293.15-298.15 K were fitted to an equation for calculating μ_r as follows:

$$\mu_r = \mathrm{D}\left(0.01106\varphi^2 + 0.04466\varphi\right) + 1.063 \quad (3b)$$

The data deviation from Eqs.(3a) and (3b) was of ±10% for the varying magnitudes of B (0.2-50) and D (1-22). As a novelty the functional relationship of $k_r = k_r(\mu_r)$ was proposed at an approximate error margin of ±11% for the used data in EG/EG-W based nanofluids as follows:

$$k_r = -0.00162\left(\mu_r\right)^2 + 0.07173\left(\mu_r\right) + 1.198 \quad (3c)$$

The estimated validity range of Eq. (3c) was: For metal oxides having an overall $d_p$range of 7 nm to 100 nm having a *T* range of 293.15-323.15 K for an extended range 0% ≤ φ ≤ 55%.Meanwhile relative density, $\rho_r$and specific heat, c_{p_r}definitions are given as follows:

$$\rho_r = \frac{\rho_{NRF}}{\rho_R}, \quad c_{p_r} = \frac{c_{p_{NRF}}}{c_{p_R}} \quad (4)$$

Pak and Cho model can be used to calculate $\rho_r$and c_{p_r}as follows:

$$\rho_r = \left(1-\varphi\right) + \frac{\rho_p}{\rho_R}\varphi \quad (5a)$$

$$c_{p_r} = \left(1-\varphi\right) + \frac{c_{p_p}}{c_{p_R}}\varphi \quad (5b)$$

In Eqs.(5a) and (5b),$\rho_p$is particle density and c_{p_p} is particle specific heat which can be taken from Table 1.

2.3 Studies on cooling system performance

Using NRF is a novel method to enhance the performance of cooling system with increased cooling capacity -COP of the system due to augmentation of thermophysical characteristics of R [47-49]. However the number of experimental and theoretical studies concentrating on the direct relevance to cooling system performancein terms of the interactive influence of the governing parameters discussed above is not enough.

Kundan and Singh [21]used NRF:(Al_2O_3 (20 nm)-R134a) for φ (0.151-0.303%). They concluded that improvement in COP was from 7.20% to 16.34% for all volume flow rates and evaporator heat fluxes at 288-290 K and 303-304 Kfor φ = 0.151%. Sharma and Rana[22]studied a hybrid sized mixture NRF: (Al_2O_3 (20-30 nm)-R134a) at φ = 0.151%. Theirresults indicated that COP_R was less than COP_{NRF}.

Kushwaha et al. [23]examined the performance of NRF: (Al_2O_3(60-70 nm)-R134a) for varying φ (0.075-0.151%). They observed that COP_{NRF} improved upto 9.14% over COP_R.In reference to the studies of Mahbubul et al. [17] and Alawi et al. [18], Table 6 can be formed.

Mahbubul et al. [17]analyzed specifically the impact of *k*, *μ*,and *ρ* NRF: (Al_2O_3-R134a) for φ = 5% at T = 283–308 K range for a uniform mass flux through a horizontal smooth tube. The analytical results showed that the COP, *k*, *μ* and *ρ* of NRF enhanced compared to those of R whereas c_p of NRF is slightly lower than that of pure R. As a similar study Alawi et al. [18]used NRF: (Al_2O_3-R-141b) for φ = 1–4% at T = 283–308 K. They concluded that there existed enhanced COP and thermophysical characteristics of NRF except for c_p of NRF which was lower than c_p of R.

Equations	Remarks
$$COP_{NRF/R} = E\left[0.023\frac{k_{NRF/R}}{d_{tube}}\text{Re}^{0.8}\text{Pr}^{0.4}\right]\frac{A\Delta T}{W_{net,in}} \\ +S\left[207\frac{k_{NRF/R}}{bd}\left(\frac{qbd}{T_s}\right)^{0.674}\left(\frac{\rho_v}{\rho}\right)^{0.581}\text{Pr}^{0.533}\right]\frac{A\Delta T}{W_{net,in}}$$	COP_{NFR} and COP_R are calculated using k_{NRF} and k_R for different T and φ. k_{NRF} is predicted using Sitprasert model. A = heat transfer area.
$$COP_{NRF/R} = E\left[\frac{0.023k_R^{0.6}}{d_{tube}}\text{Re}^{0.8}\left(c_{p_{NRF/F}}\mu_R\right)^{0.4}\right]\frac{A\Delta T}{W_{net,in}} \\ +S\left[\frac{207}{bd}\left(\frac{1}{k_R}\right)^{0.207}\left(\frac{qbd}{T_s}\right)^{0.674}\left(\frac{\rho_v}{\rho}\right)^{0.581}\left(c_{p_{NRF/R}}\mu_R\right)^{0.533}\right]\frac{A\Delta T}{W_{net,in}}$$	COP_{NFR} and COP_R are calculated using $c_{p_{NRF}}$ and c_{p_r} for different T and φ. $c_{p_{NRF}}$ is calculated using Pak and Cho model.
$$\frac{COP_{NRF/R}}{COP_{npl}} = 1-(2.37-0.047L+3.01\times10^{-4}L^2)\left(\frac{8\mu_{NRF/R}lV}{\pi P_{evap}r^4}\right)$$	npl = no pressure losses. COP_{NFR} and COP_R are calculated using μ_{NRF} and μ_R for different T and φ. μ_{NRF} is predicted using Brinkman model.
$$COP_{NRF/R} = \frac{\Delta h_E KA\sqrt{2g\rho_{NRF/R}\left(P_{up}-P_{down}\right)}}{W_{net,in}}$$	COP_{NFR} and COP_R are calculated using and ρ_R for different T and φ. ρ_{NRF} is predicted using Pak and Cho model.

Table 6: Correlations proposed by Mahbubul et al. [17] and Alawi et al. [18] for COP expressed in terms of COP_r

III. PERSPECTIVES

Theoretical and experimental research are almost of independent nature and paying particular attention to refrigeration performance with a great variety of limitations in terms of nanoparticle, R, and NRF preparation and cycle operational parameters. Therefore state of art is still far from the generalized approaches, equations and physical explanations. In fact increasing performance of a refrigeration cycle with the use of a nanorefrigerant is a fact governed by cycle-system design and strongly related to the operational conditions. However disregarding refrigeration cycle and system operational restrictions thermophysical characteristics of NRF with respect to R can be evaluated to determine the enhancement of system performance. Furthermore there exists a severe gap to install a correlation between thermophysical characteristics of NRF and COP under the influence of major preparation parameters of φ and T.

Relative unitless parameters describing the departure of NRF from R should be referred in order to provide a generalized - common base analysis. The existing parameters of varying ranges are such that they have an interactive and non-linear influence on system performance. Therefore there exists a severe difficulty with an exciting challenge to propose a general functional relationship for a NRF handling system performance. Under the light of outlined state of art following deductions can be listed:

1) Nanoparticles' thermophysical characteristics and parameters of (φ, T) have expectedly the governing influence since the same nanoparticles added in different refrigerants result in similar refrigeration system performance. Enhancement in thermophysical characteristics (k, μ, ρ, and c_p) of NRF is almost well-defined theoretically. However as a reverse matter a particular attention should be given to the experimentally observed reduction in c_p of NRF. Determination of the interactive influence of the thermophysical parameters, operational parameters on COP is a gap.

2) Experimental verification is a necessity particularly to set the influence of parameters of (φ, T). The critical parameter seems to be φ. COP value for a system using NRF: (Al_2O_3-R134a) at $\varphi = 0.151\%$ is over that of one using R whereas COP value for a system using NRF: (Al_2O_3-R134a) at $\varphi= 0.302\%$ is less than that of one using R. The functional relationship of $COP_r(\varphi)$ should be used to determine the optimum condition for φ. The optimum condition for φ also serves a solution for possible particle clogging problems in system components observed at high φ. Another disadvantage of high φ is coupled with the fact of increasing μ associated with increase in pressure drop and pumping power in turn. Therefore determination of acceptable

and efficient value of φ resulting in an increased COP without particle clogging and with acceptable pumping power of the system is a requirement.
3) Experimental and theoretical research should verify each other to reach a complete understanding of the physical mechanism of NRF in a refrigeration cycle. Stability behaviour and life time of NRF in a refrigeration cycle are the basic gaps to be fulfilled in near future.

The major attention of the paper is devoted to the determination of a general functional relationship between COP_r and the governing parameters of NRF, R, nanoparticles, φ, and governing temperatures of evaporator: T_e and ambient -reference: T_o using available experimental data and well defined theoretical calculation scheme.

A computational modeling –a correlation study resulted in the definition of Miscellaneous Multiplier, M is provided to fill the gap.

IV. COMPUTATIONAL MODELING -A CORRELATION STUDY

As a critical result of the analysis the following functional relationship can be proposed:

$$COP_r = f\left(d_p, \varphi, T_e, T_o, k_p, k_R, k_r, \mu_r, \rho_r, c_{p_r}, V\right) \text{ (6a)}$$

In Eq. (6a) refrigeration cycle operational parameters of T_e, T_o, and V are the dimensional parameters besides critical nanoparticle dimension of d_p. Cycle performance parameter COP_r and remaining parameters are dimensionless ones. It is known that k_r, μ_r, c_{p_r}, and ρ_r are under the severe influence of φ which can be described by functional relationships:

$$k_r = f(\varphi), \ \mu_r = f(\varphi), \ \rho_r = f(\varphi), \ c_{p_r} = f(\varphi) \text{ (6b)}$$

In terms of experimental research most of the attention is devoted to the functional dependence of COP_r on φ:

$$COP_r = f(\varphi) \text{ (6c)}$$

For k_r and μ_r, Eqs.(3a) and (3b) can be used. Meanwhile for c_{p_r} and ρ_r functional relationships of Pak and Cho model given in Eqs. (5a) and (5b) can be used. The confirmation of Eqs.(3a) and (3b) are checked by using available experimental data of a variety of NRF [8, 9, 10, 12, 16] and [10, 13, 14], respectively. In Fig. 1, the calculated values of k_r obtained from Eq. (3a) are in good agreement with the experimental ones for the magnitudes of B=5, B=13 and B=28.
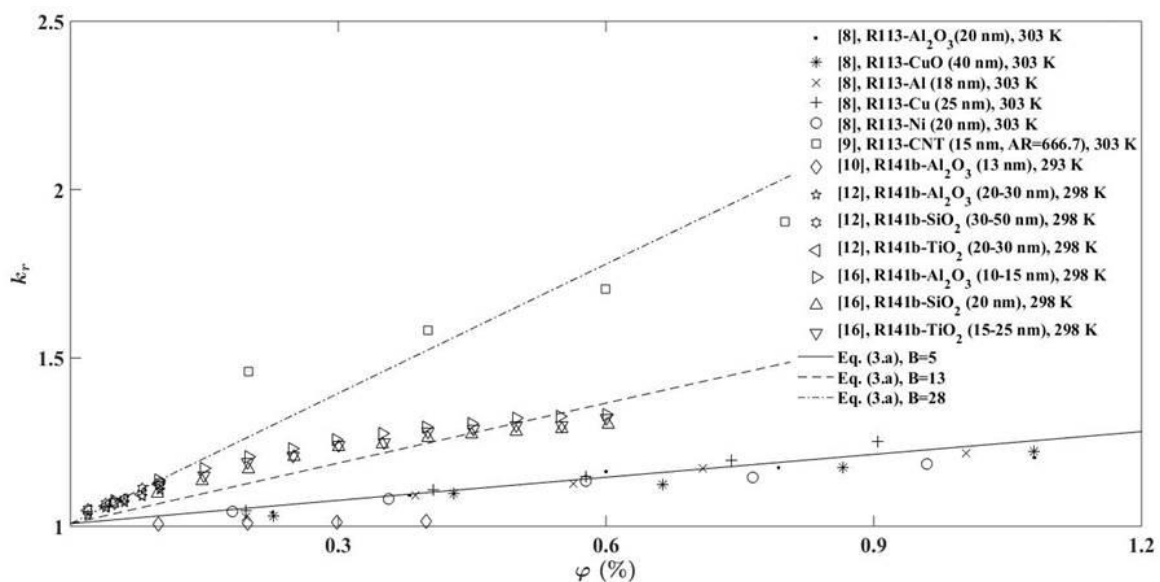

Figure 1: Functional relationship of $k_r(\varphi)$ using Eq. (3a) for NRF data

However as can be seen from Fig. 2 the calculated values of µr obtained from Eq. (3b) for the magnitude of D = 1 are not in agreement with the experimental ones. This is possibly due to the cited range of D as 1-22 in Eq. (3b). There is a severe difference between thermophysical characteristics of EG, EG-W with R11, R141b, and R123 and maximum error in the value of μ is 13% at 2% φ.
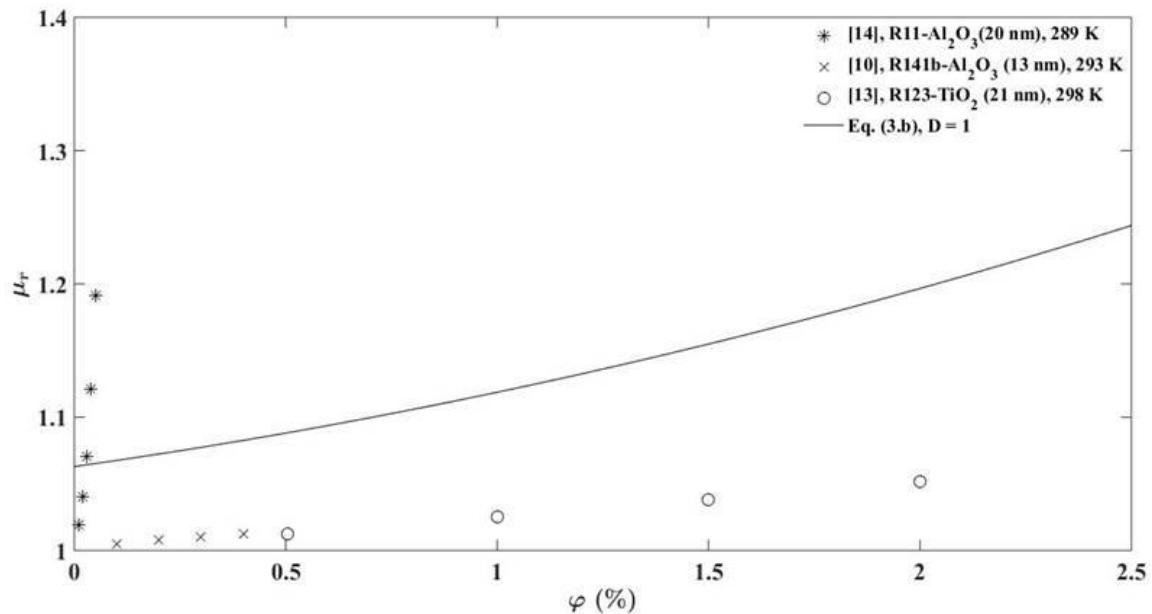

Figure 2: Functional relationship of $\mu_r(\varphi)$ using Eq. (3b) for NRF data

The experimental data gathered from references [21-23]using NRF: (Al_2O_3-R134a) for performance of refrigeration cyclesare used for the modeling study. In order to determine the proposed functional relationships of Eqs.(6a), (6b) and (6c), available experimental data are expressed in Table 7. As can be seen from Table 7, the variables are d_p, φ, V, T_o, and $T_e$in accordance with Eq. (6a). The covered ranges of experimental data are as d_p = 20-70 nm, φ= 0.075-0.303%, V= 6.5-11 liter/hour, T_o=294-306 K and T_e= 288-309 K.

References	d_p(nm)	φ(%)	V(liter/hour)	T_o(K)	T(K)	COP_{NRF}	COP_R	COP_r
[21]	20 (20*)	0.151, 0.303	6.5	294	288-290 (289*)	1.07, 0.93	0.98	1.09, 0.95
					303-304 (303.5*)	1.01, 0.89	0.93	1.09, 0.96
				301	288-290 (289*)	0.94, 0.78	0.86	1.09, 0.91
					303-304 (303.5*)	0.98, 0.86	0.91	1.08, 0.95
			11	294	288-290 (289*)	0.88, 0.74	0.77	1.14, 0.96
					303-304 (303.5*)	0.94, 0.87	0.85	1.11, 1.02
				301	288-290 (289*)	0.77, 0.62	0.66	1.17, 0.94
					303-304 (303.5*)	0.90, 0.84	0.80	1.13, 1.05
[22]	20-30 (25*)	0.151	10	298	298-299 (298.5*)	0.91	0.85	1.07
[23]	60-70 (65*)	0.075, 0.151	11	306	298-299 (298.5*)	0.68, 0.76	0.68	1.00, 1.12
				304.5	308-309 (308.5*)	0.87, 0.94	0.86	1.01, 1.09

* Average value of $d_p$and T_e used in calculations

Table 7: The calculated COP_rresults for available experimental data

The average magnitude of $d_p$is used for the calculations and $COP_r$is determined for separate cases.

The calculated number of cases is 21 for the covered range of the variables. Figures 3, 4, and 5 are formed to determine $c_{p_r}(\varphi)$, $\rho_r(\varphi)$ and $COP_r(\varphi)$ for the calculated data respectively.
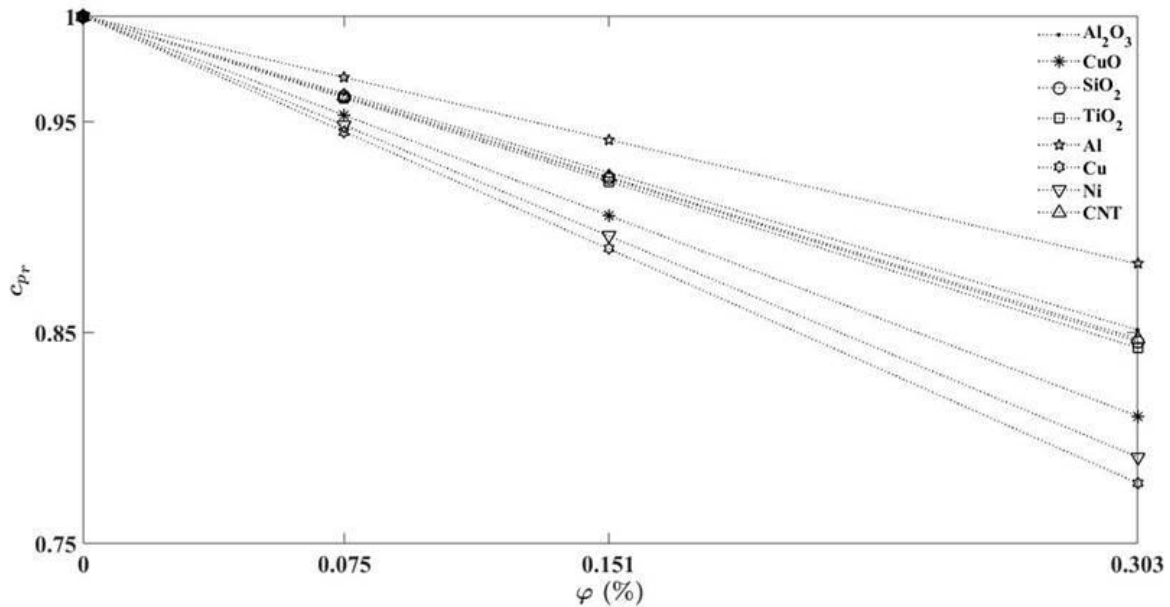
Figure 3: Functional relationship of $c_{p_r}(\varphi)$ using Pak and Cho model
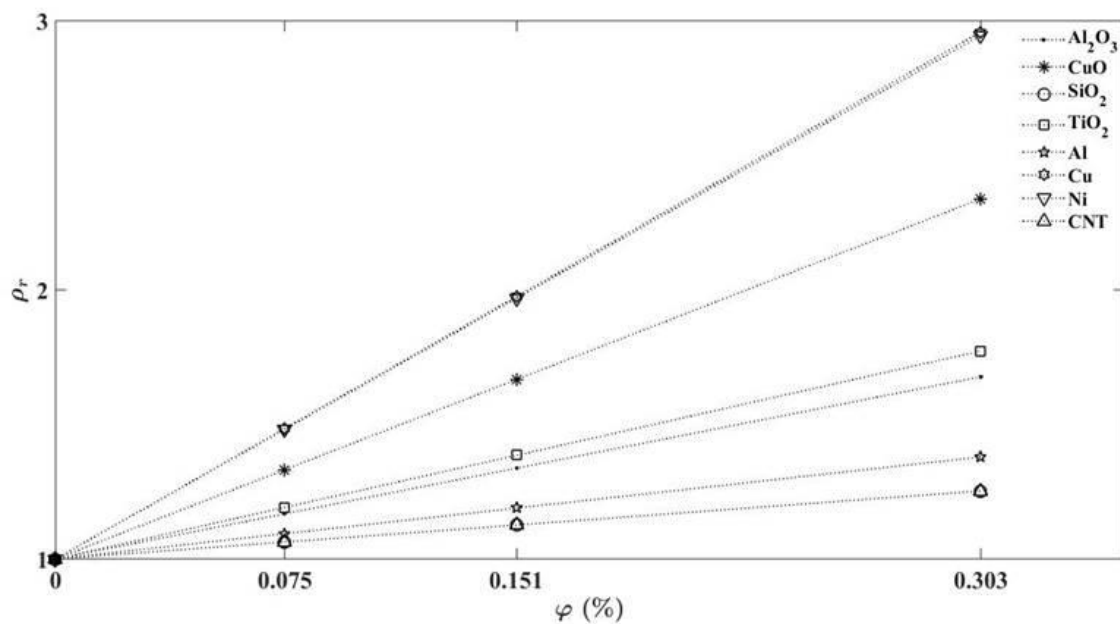

Figure 4: Functional relationship of $\rho_r(\varphi)$ using Pak and Cho model

The calculated data points are given in Fig. 5 in terms of Eq. (6c) to determine $COP_r(\varphi)$. The influence of the parameters φ, T_e, T_o, d_p, and V given in Eq. (6a) is apparent. However influence of basic thermophysical characteristics are not seen clearly. The maximum COP_r is obtained with d_p= 20 nm, V = 6.5 liter/hour, T_o = 294 K, and T_e= 288-290 K. COP_r maximum is fitted with φ <0.151%. COP_r increases with φ for an increase of φ for $\varphi < 0.151\%$ meanwhile for $\varphi > 0.151\%$ COP_r decreases having a minimum value at $\varphi = 0.303\%$. This means that φ is the governing parameter and the optimum condition is related to the magnitude of φ. The relationship between COP_r and φ is not a linear one.

The exact form of the functional relationship of Eq. (6c) is estimated to fit the experimental data by means of a second degree polynomial using MATLAB Curve Fitting Toolbox.
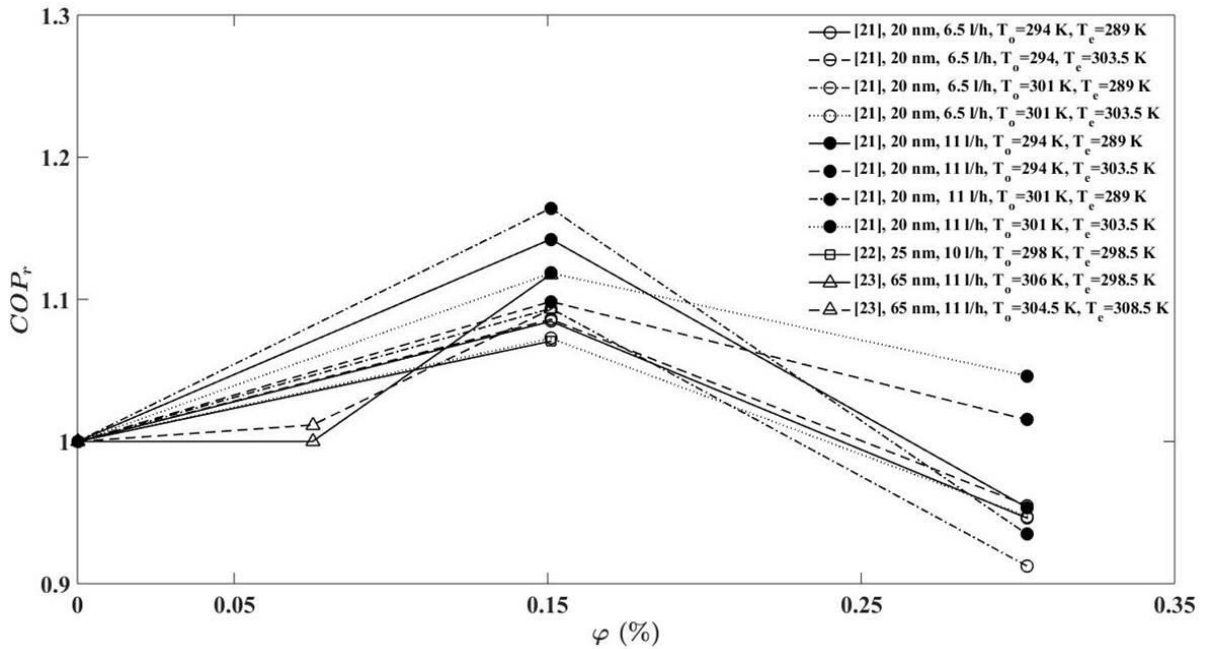
Figure 5: Presentation of Table 7 data in terms of $COP_r(\varphi)$

The solid line drawn in Fig. 6 is given by Eq. (7) as follows:

$$COP_r = -4.967(\varphi)^2 + 1.408(\varphi) + 1 \quad (7)$$

The prediction bounds of experimental data are given with a confidence level of 95%. Eq. (7) is satisfying the boundary condition of $\varphi = 0\%$ resulting in $COP_r = 1$.
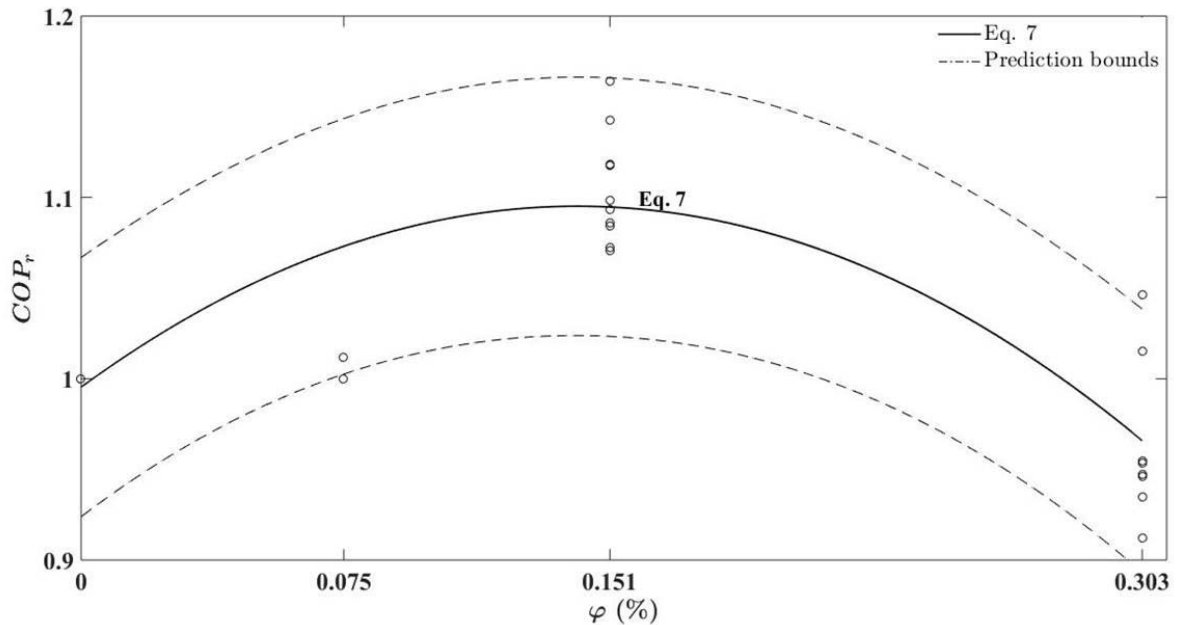

Figure 6: The fitted curve for COP_r as a function φ (%)

Disregarding the utilized data range of Fig. 1, Fig. 2, Fig. 3, and Fig. 4 the validity of the functional relationships k_r, μ_r, c_{p_r} and ρ_r in Eq. (6b) is a fact. Eq. (6c) of $COP_r(\varphi)$ is also well defined with Fig. 6.

In order to find the interactive influence of the remaining parameters of Eq. (6a); d_p, k_p, k_R, T_e, T_o, V, k_r, μ_r, c_{p_r} and ρ_r on COP_r, a trial and error procedure is followed. Therefore the experimental data are expressed in terms of plots having φ as the dominant variable. Since the variation of φ causes variation in

thermophysicalcharacteristics of NRF. In this respect following functional relationship is suggested as a first trial letting a constant value of V. In reference totalized data of V in the range of 6.5–11 liter/hour, 95% confidence of data with Eq. (7) means that the influence of V is not critical.

$$\text{COP}_r = f\left(h/d_p, \varphi, T_o/T_e, k_p/k_R, k_r, \mu_r, \rho_r, c_{p_r}\right) \quad (8a)$$

In Eq. (8a), unitless parameters are referred. $d_p$is expressed unitless by using h; capping layer thickness. The capping layer was introduced by Hosseini et al.[50]as an important correlation parameter for several nanofluid applications. Capping layer thickness, h was taken as 1 nm for predicting k_r and μ_r [49, 51]. Since $\text{COP}_r = f(\varphi)$ is well defined with Eq. (6c) and Eq. (7), the estimated functional relationship of Eq. (8a) is given by a plot of $\text{COP}_r(h/d_p, T_o/T_e, k_p/k_R, k_r, \mu_r, c_{p_r}, \rho_r)$ in Fig. 7.
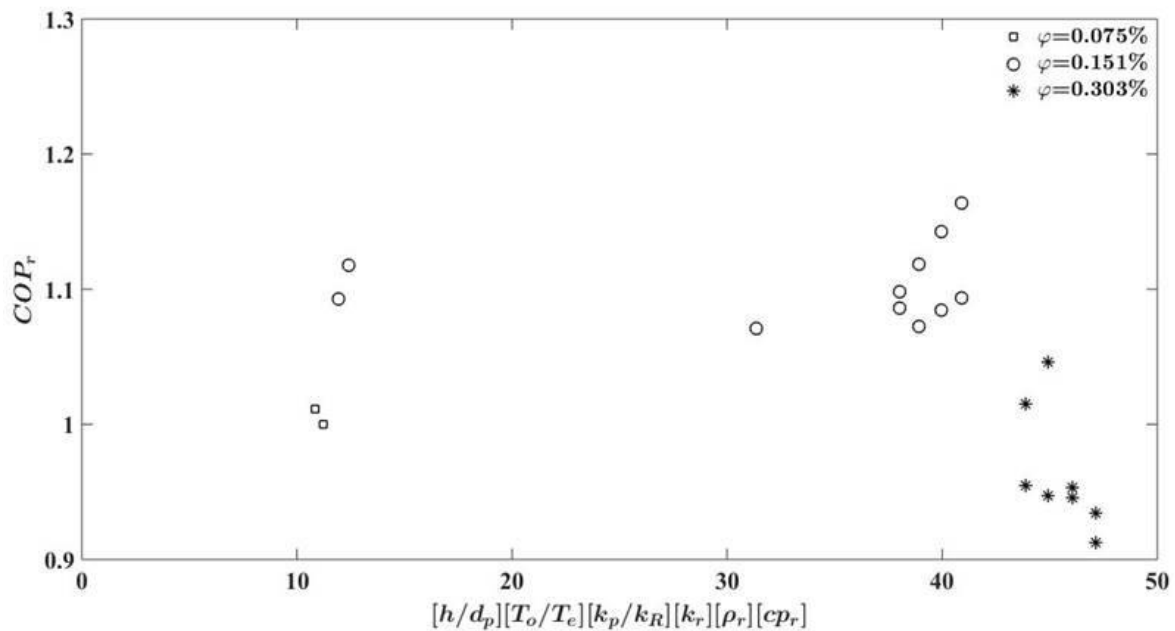
Figure 7: The first trial plot to determine the influence of the available parameters on COP$_r$

The multiplication of the functional dependence parameters are given in the abscissa with corresponding COP$_r$ in ordinate. The data points are shown with φ as a variable.As can be seen from Fig.7 governing effect of φ is clear. The data corresponding to $\varphi = 0.151\%$ are almost independent of the multiplication parameters in the abscissa taking a value of COP$_r$ in the order of 1.1.

On the other hand the data corresponding to $\varphi = 0.303\%$ has a dependence on the multiplication parameters in the abscissa with COP$_r$ values ranging between 1.05-0.9 approximately. The data corresponding to $\varphi = 0.075\%$ have COP$_r$ =1 roughly.As denoted in the discussion above optimum value of $\varphi = 0.151\%$ (Fig. 6) is apparent since for a great range of the multiplication parameters in the abscissa (between10-40) COP$_r$ is approximately 1.1. This means that an optimum value of φ exists for which COP$_r$ is almost independent of the parameters of Eq. (8a).As a second trial following functional relationship using estimated exponents of the multiplication parameters of Eq. (8a) is suggested as an outcome of tedious calculations:

$$\text{COP}_r = f\left(\left[h/d_p\right]^{1.95}, \left[T_o/T_e\right]^{5.5}, \left[\ln\left(k_p\right)/k_R\right]^{1.45}, \left[k_r\right], \left[\rho_r\right]^{0.5}, \left[c_{p_r}\right]\right) \quad (8b)$$

The estimated functional relationship of Eq. (8b) is given by a plot of $\text{COP}_r(\left[h/d_p\right]^{1.95}\left[T_o/T_e\right]^{5.5}\left[\ln(k_p)/k_R\right]^{1.45}\left[k_r\right]\left[\rho_r\right]^{0.5}\left[c_{p_r}\right])$ in Fig. 8.
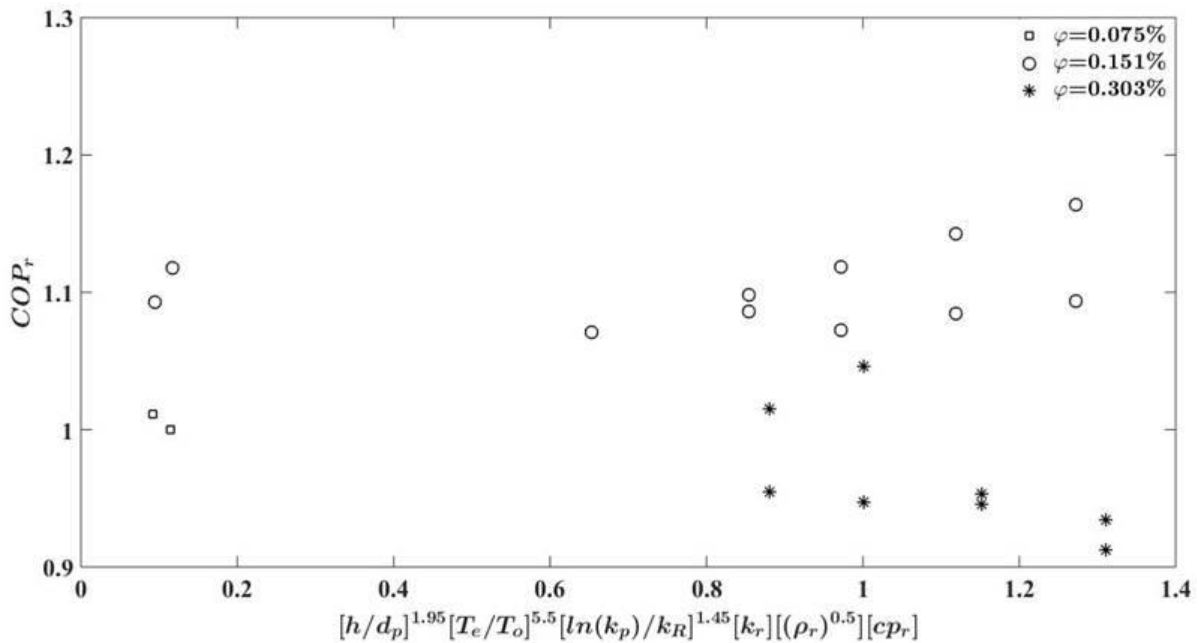
Figure8: The second trial plot for suggested Eq. (8b)

The multiplication of the functional dependence parameters are given in the abscissa with corresponding COP_r in the ordinate. The data points are shown with φ as a variable.The behaviour of data points in Fig. 8 is such that suggested Eq. (8b) is well defined with the previous reasoning on φ. However the data points corresponding to different φ are close to each other indicating the possibility of a single relationship for $COP_r([h/d_p]^{1.95}[T_o/T_e]^{5.5}[\ln(k_p)/k_R]^{1.45}[k_r][\rho_r]^{0.5}[c_{p_r}])$ under the influence of φ.

V. MISCELLANEOUS MULTIPLIER, M

As a resulting trial to express the interactive influence of the unitless parameters $[h/d_p]^{1.95}[T_o/T_e]^{5.5}[\ln(k_p)/k_R]^{1.45}[k_r][\rho_r]^{0.5}[c_{p_r}]$ and φ on COP_ra unitless parameter M called as Miscellaneous Multiplier is defined as follows:

$$M = \left[h/d_p\right]^{1.95}\left[T_o/T_e\right]^{5.5}\left[\ln\left(k_p\right)/k_R\right]^{1.45}\left[k_r\right]\left[\rho_r\right]^{0.5}\left[c_{p_r}\right]\left[-4.967(\varphi)^2 + 1.408(\varphi)\right] \quad (9a)$$

Miscellaneous Multiplier includes nanoparticle, R, NRF and refrigeration cycle operational parameters with the governing influence of φ. In definition φ is sensed by taking the following term from Eq. (7) as a multiplication parameter:

$$COP_r - 1 = \left[-4.967(\varphi)^2 + 1.408(\varphi)\right] \quad (9b)$$

Therefore COP_rcan be expressed as a function of Miscellaneous Multiplier, M.

$$COP_r = f(M) \quad (9c)$$

As a third trial to express $COP_r(M)$, Fig. 9 is installed. As can be noticed from Fig. 9, $COP_r(M)$ can be described by an equation:

$$COP_r = 1.025 + 1.615M - 7.537M^2 \quad (10)$$

The data corresponding to all φ magnitudes are in well correspondence with Eq. (10) verifying the correctness and utility of M.As can be seen from Fig. 9, M varies between -0.05–0.15. COP_r is less than 1 in the range of M<0.

Although the data points with $COP_r < 1$ with $M < 0$ are for $\varphi = 0.303\%$ as a general deduction they are also in obedience to Eq. (10). This means that M is well fitted to the data behaviour independent of φ.
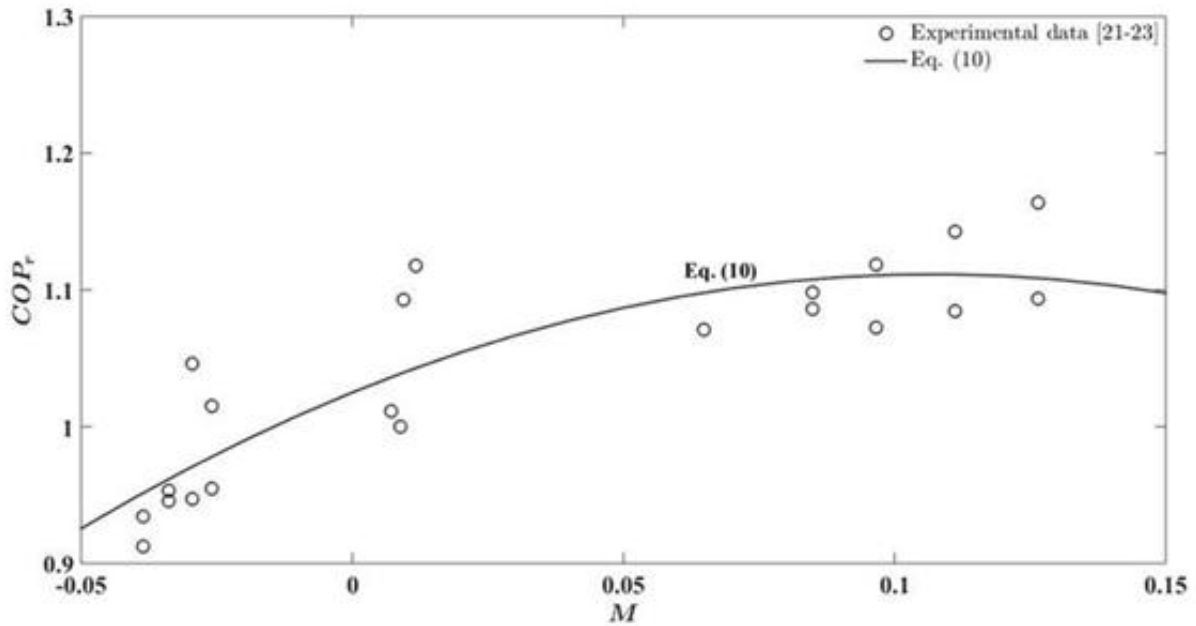

Figure9: Proposed COP_r(M) relationship verifying the correctness of Miscellaneous Multiplier

The novelty of the Eq. (10) is such that the interactive influence of the listed parameters can be determined with a resulting calculation of COP_r. M can be calculated with varied magnitudes of the parameters and /or for a required COP_r the magnitudes of individual parameters can be estimated. The limiting situation for $COP_r = 1$ can be determined with the magnitude of M. Therefore the magnitude of each parameter in M can be set to reach the aimed COP_r. The definition and utility of Miscellaneous Multiplier for the calculation and /or estimation of the relevant parameters for a required COP_r seems a great contribution to the state of art since Miscellaneous Multiplier takes into account all of the parameters including operational limitations.The validity of Eq. (10) with experimental data is given in Fig. 10.
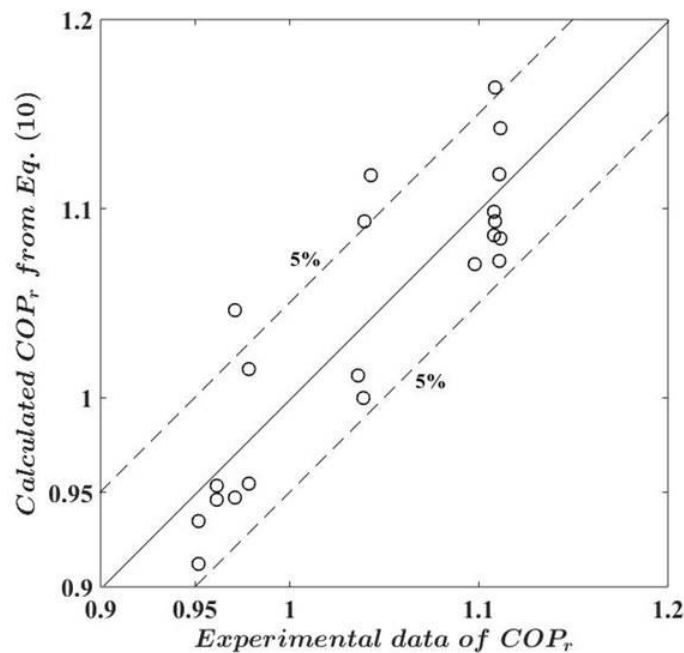

Figure 10: COP_r calculated by Eq. (10) as a function of experimental COP_r for Al_2O_3-R134a NRF

The satisfaction of experimental data is acceptable with ±5% of deviation.In order to complete the physical reasoning on the utility of M and its dependence on COP_r through Eq. (10) further calculations of modeled cases are conducted and Fig. 11 through Fig. 13 are constructed.
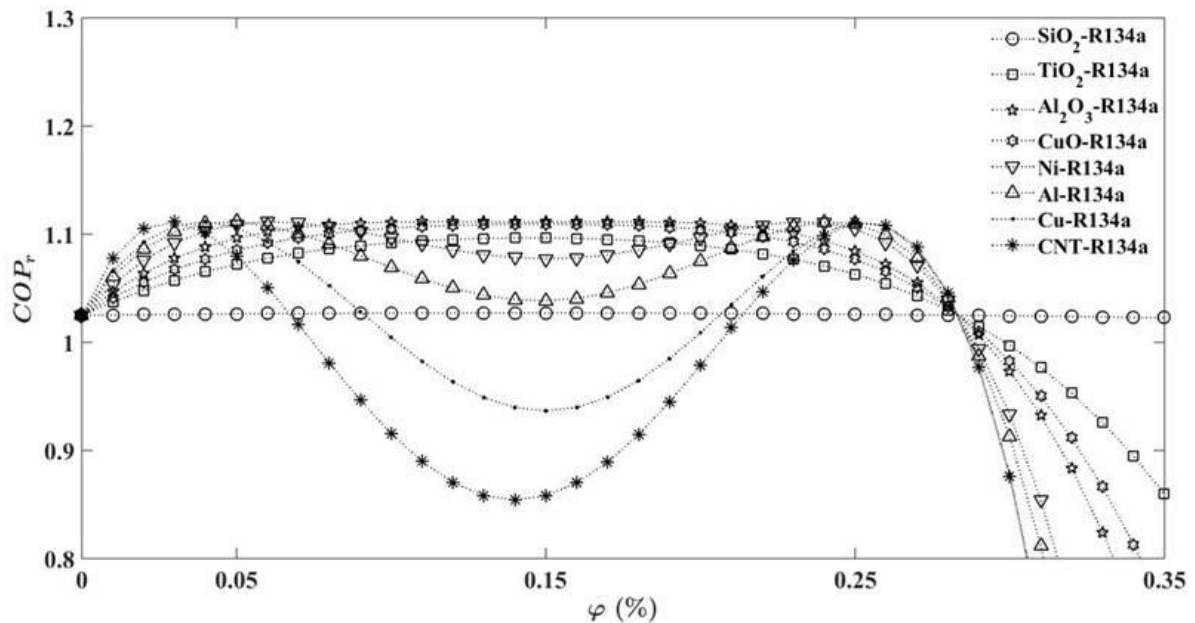

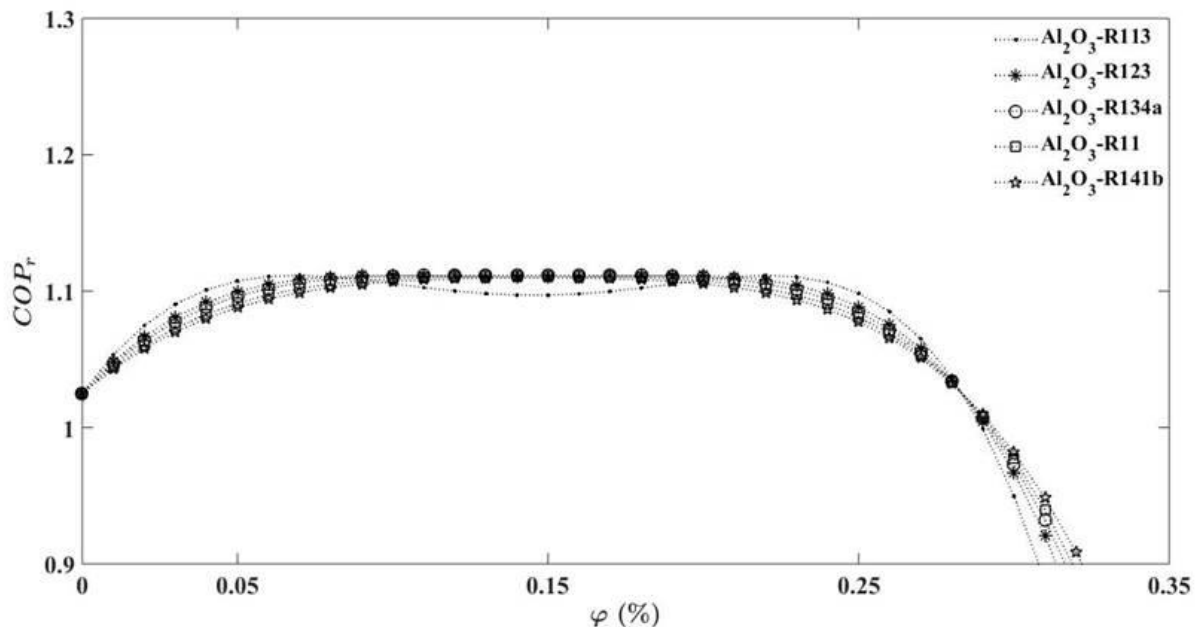**Figure 11: Influence of nanoparticles for COP_r(M) calculation by Eq. (10)**

Figure 12: Influence of refrigerants for COP_r(M) calculation by Eq. (10)

Figure 11 is formed with the calculated COP_r of R134a based NRF with different nanoparticles using Eq. (10) for d_p= 20 nm, T_o = 294 K and T_e = 289 K. Figure 12 is formed with the calculated COP_r of NRF with different refrigerants using Eq. (10) for d_p = 20 nm Al_2O_3, T_o = 294 K, and T_e= 289 K. Figure 13 is formed with the calculated COP_r of NRF: (Al_2O_3 (20nm)-R134a) with different T_e using Eq. (10) for d_p= 20 nm Al_2O_3, T_o = 294 K.As can be seen from Fig. 11, in R134a COP_r of SiO_2 is independent of φ. COP_r of Al_2O_3, TiO_2, CuO, and Ni have a similar dependence on φ. Inside the approximate range of 0.025% $<\varphi$ <0.26% COP_r takes a constant value of 1.1. COP_r of Al, Cu, and CNT have similar behaviour departing from the other nanoparticles such that the maximum COP_r=1.1 is obtained at φ = 0.025% and φ = 0.26% meanwhile at φ = 0.15% there is a reduction in COP_r. COP_r = 1 roughly for Al, COP_r= 0.95 for Cu and COP_r= 0.85 for CNT corresponding to φ = 0.15%.

This data behaviour implies that the influence of thermophysical characteristics of nanoparticles is governing the relationship of $COP_r(\varphi)$. This fact is also sensed in Fig. 12 since the presence of the same nanoparticle Al_2O_3 in a variety of refrigerants result in almost the same $COP_r(\varphi)$.
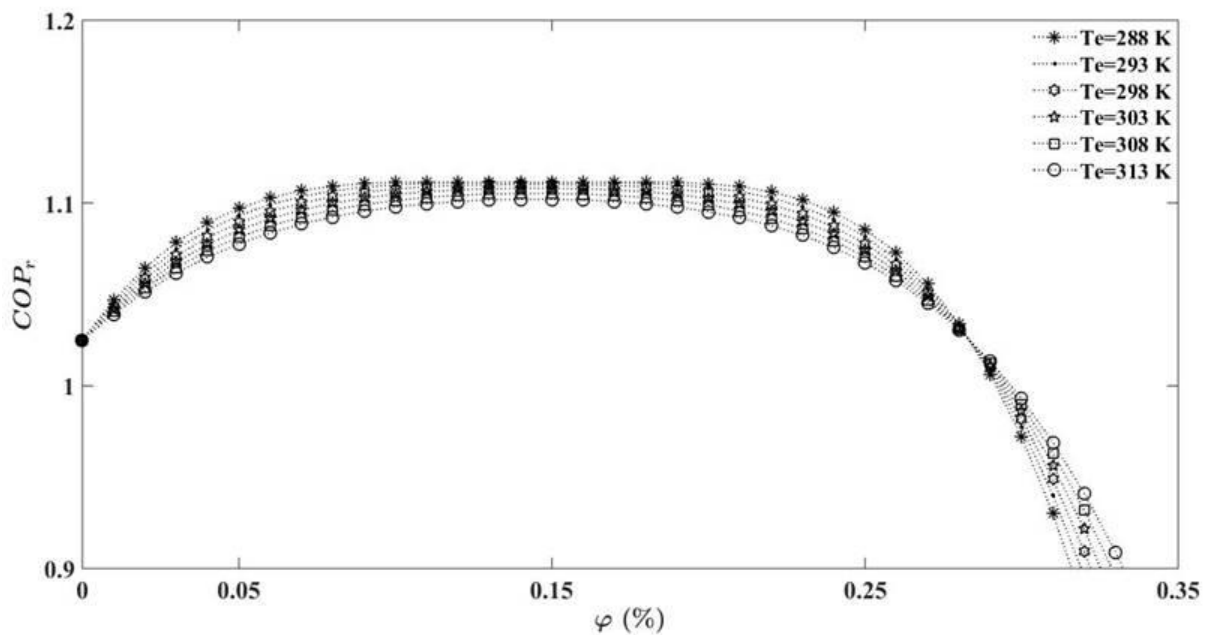

Figure 13: Influence of T_e for COP_r (M) calculation by Eq. (10)

Furthermore as can be seen from Fig. 13 decreasing T_e has a positive effect on COP_r. However the magnitude of φ has a serious influence on data behaviour. Since at $\varphi = 0.025\%$ and at $\varphi = 0.275\%$ COP_r is the same for all T_e indicating T_e independence for COP_r.

VI. CONCLUDING REMARKS

The current study of Moshfeghi and Toghraie[52] presenting an overall updated review on the rheological behavior of nanofluids and the similar research selected as samples ones of Żyla and Fal[53], Alirezaie et al. [54], Esfe et al. [55], Moldoveanu et al. [56], Esfe et al.[57], Esfe[58] and Kumar et al. [59] on a variety of engineering applications with nanofluids are verifying the ongoing necessity of research on nanofluids.

The particular emphasis devoted to refrigeration performance of nanofluids called as NRF is the topic of the present paper in relevance to the state of art. Therefore state of art and perspectives on nanorefrigerants are outlined. A computational modeling study in terms of functional correlations of defined parameter sets is provided. In reference to the available experimental data a tedious correlation study is conducted to provide a link between COP_{NRF} and thermophysical characteristics of NRF. The introduced unitless Miscellaneous Multiplier, M and the equation of COP_r(M) are the basic outcomes of the study. The influence of thermophysical characteristics of nanoparticles, refrigerants and refrigeration cycle operational parameters are included in a single functional relationship, COP_r(M) for the first time as a solid contribution.

The following results derived from the applied ranges of the parameter sets are the concluding phrases of the study:

i) The validity of proposed equations $COP_r(\varphi)$ and COP_r(M) are found acceptable in a $\pm 5\%$ maximum deviation of the experimental data independent of the amount of circulating NRF, V.

ii) The governing parameters for description of refrigeration performance are φ, type–thermophysicalcharacteristics of nanoparticles which in turn magnitude of M through COP_r(M).

iii) The optimum range of φ is estimated to be $0.025\% < \varphi < 0.26\%$.

REFERENCES

[1].   Kaplan M. and Carpinlioglu M.O., 2019. An Extensive Review on Nanofluids - Based on Available Experimental Studies. Proceedings of 2nd International Symposium on Innovative Approaches in Scientific Studies, pp. 104-116.

[2].   Celen A., Çebi A., Aktas M., Mahian O., Dalkilic A.S. and Wongwises S.,2014. A review of nanorefrigerants: flow characteristics and applications. International Journal of Refrigeration, 44: 125-140.

[3]. Alawi O.A., Sidik N.A.C. and Mohammed H.A., , 2014. A comprehensive review of fundamentals, preparation and applications of nanorefrigerants. International Communications in Heat and Mass Transfer, 54: 81-95.

[4]. Redhwan A.A., Azmi W.H., Sharif M.Z. and Mamat R., 2016. Development of nanorefrigerants for various types of refrigerant based: a comprehensive review on performance. International Communications in Heat and Mass Transfer, 76: 285-293.

[5]. Kasaeian A., Hosseini S.M., Sheikhpour M., Mahian O., Yan W.M. and Wongwises S.,2018 Applications of eco-friendly refrigerants and nanorefrigerants: a review. Renewable and Sustainable Energy Reviews, 96: 91-99.

[6]. Bhattad A., Sarkar J. and Ghosh P., 2018. Improving the performance of refrigeration systems by using nanofluids: a comprehensive review. Renewable and Sustainable Energy Reviews, 82: 3656-3669.

[7]. Sharif M., Azmi W.H., Mamat R., Shaiful A.I.M., Mechanism for improvement in refrigeration system performance by using nanorefrigerants and nanolubricants: a review. International Communications in Heat and Mass Transfer, 2018, 92: 56–63.

[8]. JiangW., DingG., PengH., GaoY., and WangK., 2009. Experimental and model research on nanorefrigerant thermal conductivity. HVAC&R Research, 15(3): 651–669.

[9]. Jiang W., Ding G. and Peng H., 2009. Measurement and model on thermal conductivities of carbon nanotube nanorefrigerants. International Journal of Thermal Sciences, 48(6): 1108–1115.

[10]. Mahbubul I.M., Saidur R. and Amalina M.A.,2013. Thermal conductivity, viscosity and density of R141b refrigerant based nanofluid. Procedia Engineering, 56: 310–315.

[11]. Mahbubul I.M., Saidur R. and Amalina M.A.,2013. Influence of particle concentration and temperature on thermal conductivity and viscosity of Al2O3/R141b nanorefrigerant. International Communications in Heat and Mass Transfer, 43: 100–104.

[12]. Zhang S., Yu Y., Xu Z., Huang H., Liu Z., Liu C., Long X. and Ge Z., 2020. Measurement and modeling of the thermal conductivity of nanorefrigerants with low volume concentrations. ThermochimicaActa, 178603.

[13]. Mahbubul I.M., Saidur R. and Amalina M.A.,2012. Investigation of viscosity of R123-TiO2 nanorefrigerant. International Journal of Mechanical and Materials Engineering, 7(2): 146–151.

[14]. Dhindsa G.S. and Kundan L.,2013. Experimental investigation of the viscous behavior of Al2O3 based nanorefrigerant. International Journal on Theoretical and Applied Research in Mechanical Engineering, 2(3): 143-147.

[15]. Alawi O.A. and Sidik N.A.C.,2014. Influence of particle concentration and temperature on the thermophysical properties of CuO/R134 a nanorefrigerant. International Communications in Heat and Mass Transfer, 58: 79–84.

[16]. Zhang S., Li Y., Xu Z., Liu C., Liu Z., Ge Z. and Ma L.,2022. Experimental investigation and intelligent modeling of thermal conductivity of R141b based nanorefrigerants containing metallic oxide nanoparticles. Powder Technology, 395: 850-871.

[17]. Mahbubul I.M., Saddah A., Saidur R., Khairul M.A. and Kamyar A., 2015. Thermal performance analysis of Al2O3/R-134a nanorefrigerant. International Journal of Heat and Mass Transfer, 85: 1034–1040.

[18]. Alawi O.A., Salih J.M. and Mallah A.R.,2019. Thermo-physical properties effectiveness on the coefficient of performance of Al2O3/R141b nano-refrigerant. International Communications in Heat and Mass Transfer, 103: 54–61.

[19]. Alawi O.A. and Sidik N.A.C., 2015. The effect of temperature and particles concentration on the determination of thermo and physical properties of SWCNT-nanorefrigerant. International Communications in Heat and Mass Transfer, 67: 8-13.

[20]. Molana M. and Wang H.A., 2020. A critical review on numerical study of nanorefrigerant heat transfer enhancement. Powder Technology, 368: 18-31.

[21]. Kundan L. and Singh K., 2020. Improved performance of a nanorefrigerant-based vapor compression refrigeration system: a new alternative, Proceedings of the Institution of Mechanical Engineers, Part A: Journal of Power and Energy, 235: 106–123.

[22]. Sharma T. and Rana L.K.,2015. An experimental investigation of nano refrigerant based refrigeration system. International Journal of Electrical and Computer Engineering Systems, 4, 317–322.

[23]. Kushwaha P.K., Shrivastava P. and Shrivastava A.K., 2016. Experimental study of nanorefrigerant (R134a + Al2O3) based on vapor compression refrigeration system, International Journal of Mechanical and Production Engineering, 4(3): 90–95.

[24]. Aktas S., Dalkilic A.S., Celen A., Cebi A., Mahian O. and Wongwises S.,2015. A theoretical comparative study on nanorefrigerant performance in a single-stage vapor-compression refrigeration cycle. Advances in Mechanical Engineering, 7(1): 138725.

[25]. Zarma I.H., Ahmed M. and Ookawara S., 2019. Enhancing the performance of concentrator photovoltaic systems using nanoparticlephase change material heat sinks, Energy Conversion and Management, 179: 229–242.

[26]. Reddy M.C.S. and Rao V.V.,, 2013. Experimental studies on thermal conductivity of blends of ethylene glycol-water-based TiO2 nanofluids. International Communications in Heat and Mass Transfer, 46: 31–36.

[27]. Murshed S.M.S.,2012. Simultaneous measurement of thermal conductivity, thermal diffusivity, and specific heat of nanofluids. Heat Transfer Engineering, 33(8): 722–731.

[28]. Lahari M.L.R.C., SaiP.H.V.S.T., Narayanaswamy K.S. and Sharma K.V., 2021. Thermophysical properties of copper and silica nanofluids in glycerol-water mixture base liquid. Journal of Thermodynamics & Catalysis, 12(1): 1–11.

[29]. Salehi N., LavasaniA.M., Mehdipour R. and Yazdi M.E., 2021. Effect of nano fluids on the thermal performance and efficiency of linear fresnel collector in hot summer months. Journal of Renewable Energy and Environment, 8(4): 42-51.

[30]. Diao Y.H., Zhao T.H. and Wang Q.L., 2007. Photographic study of bubble dynamics for pool boiling of refrigerant R11. Heat and Mass Transfer, 43: 935–947.

[31]. Alawi O.A., Sidik N.A.C. and Kherbeet A.S.,2015. Measurements and correlations of frictional pressure drop of TiO2/R123 flow boiling inside a horizontal smooth tube. International Communications in Heat and Mass Transfer, 61: 42-48.

[32]. Mahbubul I.M., Fadhilah S.A., Saidur R., Leong K.Y. and Amalina M.A., 2013. Thermophysical properties and heat transfer performance of Al2O3/R-134a nanorefrigerants, International Journal of Heat and Mass Transfer, 57(1): 100-108.

[33]. Soliman A.M.A., Rahman A.K.A. and Ookawara S.,2019. Enhancement of vapor compression cycle performance using nanofluids, Journal of Thermal Analysis and Calorimetry, 135: 1507–1520.

[34]. Yang L., Xu J., Duand K. and Zhang X.,2017. Recent developments on viscosity and thermal conductivity of nanofluids, Powder Technology, 317: 348–369.

[35]. Nair V., Tailor P.R. and Parekh A.D., 2016. Nanorefrigerants: a comprehensive review on its past, present and future. International Journal of Refrigeration, 67: 290-307.

[36]. Sanukrishna S.S., Shafi M., Murukan M. and Prakash M.J.,2019. Effect of SiO2 nanoparticles on the heat transfer characteristics of refrigerant and tribologicalbehaviour of lubricant. Powder Technology, 356: 39-49.

[37]. Pak B.C. and Cho Y.I., 1998. Hydrodynamic and heat transfer study of dispersed fluids with submicron metallic oxide particles, Experimental Heat Transfer, 11(2): 151–170.

[38]. Maxwell J.A., Treatise on Electricity and Magnetism, Oxford University Press, Cambridge, UK., 1998.

[39]. Koo J. and Kleinstreuer C., 2005. Laminar nanofluid flow in micro-heat sinks. International Journal of Heat and Mass Transfer, 48(13): 2652–2661.

[40]. Sitprasert C., Dechaumphai P. and Juntasaro V., 2009. A thermal conductivity model for nanofluids including effect of the temperature-dependent interfacial layer. Journal of Nanoparticle Research, 11: 1465-1476.

[41]. A. Einstein, 1906. Eineneuebestimmung der moleküldimensionen. Annalen der Physik,324: 289–306.

[42]. Brinkman H.C., 1952. The viscosity of concentrated suspensions and solutions. Journal of Chemical Physics, 20: 571–581.

[43]. Batchelor G.K.,1977. The effect of Brownian motion on the bulk stress in a suspension of spherical particles. Journal of Fluid Mechanics, 83: 97–117.

[44]. Chen H., Ding Y. and Tan C., 2007. Rheological behaviour of nanofluids. New Journal of Physics, 9(10): 367.

[45]. Tiwari R.K. and Das M.K., 2007. Heat transfer augmentation in a two-sided lid-driven differentially heated square cavity utilizing nanofluids. International Journal of Heat and Mass Transfer, 50(9): 2002–2018.

[46]. M.O. Carpinlioglu and M. Kaplan, 2021. A correlation approach for the calculation of thermal conductivity of nanofluids as a function of dynamic viscosity, Journal of the Brazilian Society of Mechanical Sciences and Engineering, 43(5): 242.

[47]. Azmi W.H., Sharif M.Z., Yusof T.M., Mamat R. and Redhwan A.A.M.,2017. Potential of nanorefrigerant and nanolubricant on energy saving in refrigeration system — a review. Renewable and Sustainable Energy Reviews, 69: 415-428.

[48]. Yıldız G., Agbulut U. and Gürel A.E.,2021. A review of stability, thermophysical properties and impact of using nanofluids on the performance of refrigeration. International Journal of Refrigeration, 129: 342-364.

[49]. Kumar R., Singh D.K. and Chander S., 2022. A critical review on the effect of nanorefrigerant and nanolubricant on the performance of heat transfer cycles, Heat and Mass Transfer.

[50]. Hosseini S.M., Moghadassi A. and Henneke D.E., 2010. A new dimensionless group model for determining the viscosity of nanofluids. Journal of Thermal Analysis and Calorimetry, 100(3): 873–877.

[51]. Kaplan M. and Carpinlioglu M.O., 2021. Proposed new equations for calculation of thermophysical properties of nanofluids, International Advanced Researches and Engineering Journal, 5(2): 142-151.

[52]. Moshfeghi R. and Toghraie D., 2022. An analytical and statistical review of selected researches in the field of estimation of rheological behavior of nanofluids. Powder Technology, 398: 117076.

[53]. Żyła G. and Fal J., 2017. Viscosity, thermal and electrical conductivity of silicon dioxide–ethylene glycol transparent nanofluids: an experimental studies. ThermochimicaActa 650: 106–113.

[54]. Alirezaie A., Hajmohammad M.H., Ahangar M.R.H. and Esfe M.H.,2018. Price-performance evaluation of thermal conductivity enhancement of nanofluids with different particle sizes. Applied Thermal Engineering, 128: 373-380.

[55]. Esfe M.H., Bahirae M. and Mahian O., 2018. Experimental study for developing an accurate model to predict viscosity of CuO–ethylene glycol nanofluid using genetic algorithm based neural network. Powder Technology, 338: 383-390.

[56]. Moldoveanu G.M., Minea A.A., Iacob M., Ibanescu C. and Danu M., 2018. Experimental study on viscosity of stabilized Al2O3, TiO2 nanofluids and their hybrid, ThermochimicaActa, 659: 203–212.

[57]. Esfe M.H., Raki H.R., Emami M.R.S. and Afrand M., 2019. Viscosity and rheological properties of antifreeze based nanofluid containing hybrid nano-powders of MWCNTs and TiO2 under different temperature conditions. Powder Technology, 342: 808-816.

[58]. M.H. Esfe, 2019. On the evaluation of the dynamic viscosity of non-Newtonian oil based nanofluids experimental investigation, predicting, and data assessment. Journal of Thermal Analysis and Calorimetry, 135: 97–109.

[59]. R. Kumar, D.K. Singh, S. Chander,2020. An experimental approach to study thermal and tribology behavior of LPG refrigerant and MO lubricant appended with ZnO nanoparticles in domestic refrigeration cycle, Heat and Mass Transfer, 56: 2303–2311.